MATERIALS ENGINEERING

Mechanical, physical and thermoacoustic properties of lightweight composite geopolymers

INGENIERÍA DE MATERIALES

Propiedades mecánicas, físicas y termoacústicas de geopolímeros compuestos aligerados

Mónica A. Villaquirán-Caicedo[1§] iD **, Vilmary N. Perea[1]** iD **, Jhon E. Ruiz[1]** iD **, Ruby Mejía de Gutiérrez[1]** iD

[1]Universidad del Valle, Facultad de Ingeniería, Escuela de Ingeniería de Materiales, Grupo de Materiales Compuestos – Centro de Excelencia de Nuevos Materiales (CENM), Cali, Colombia

[§]*monica.villaquiran@correounivalle.edu.co, vilmary.perea@correounivalle.edu.co,*
jhon.esteban.ruiz@correounivalle.edu.co, ruby.mejia@correounivalle.edu.co

Abstract

This research evaluates the physical and mechanical properties of particulate composites, produced from geopolymer paste with the incorporation of different organic type wastes as expanded polystyrene (EP), corkwood (CK), tire rubber (RB); in percentages by volume of 2, 4, and 6%. Metakaolin was used as a precursor of the geopolymer produced by alkali activation from NaOH and sodium silicate. The geopolymer composites were cured at room temperature. Properties as density, porosity, absorption, compressive strength, thermal conductivity, and acoustic behavior were evaluated. As complementary techniques, light and scanning electron microscopy were used. It was observed that the high alkalinity of the geopolymer mixture causes deterioration of the CK particles. Composites with the incorporation of 4% of the EP and RB particles reported compressive strength of 32 and 45 MPa at 28 days, and apparent density of 1853 and 1922 kg/m^3, respectively, which represents a reduction of 6.08% and 2.58% in comparison to the GP reference. The thermal conductivity for composites with 4% of EP and RB was 0.316 and 0.344 W/m.K and the sound absorption coefficient was evaluated at frequencies of 500 Hz, 0.70, and 0.50 respectively. The evaluated performance properties show the feasibility of using 4% of EP and RB for the manufacture of geopolymer composites for applications in thermal and sound insulating panels.

Keywords: corkwood, expanded polystyrene, geopolymer, rubber wastes, thermoacoustic insulator.

Resumen

Esta investigación evalúa las propiedades físicas, mecánicas y termoacústicas de materiales compuestos particulados de matriz geopolimérica con incorporación de partículas orgánicas proveniente de residuos como poliestireno expandido (EP), madera (CK) y residuos de llantas (RB), en porcentajes de 2, 4 y % en volumen. Metakaolin fue usado como precursor del geopolímero producido por activación con NaOH y silicato de sodio. Los materiales fueron obtenidos a temperatura ambiente. Propiedades como densidad, porosidad, absorción, resistencia a la compresión, y medidas de conductividad térmica y propiedades acústicas fueron evaluadas en los compuestos desarrollados. Complementariamente fueron realizadas observaciones en microscopio óptico y electrónico. Los resultados mostraron que la alta alcalinidad de la matriz geopolimérica deteriora las partículas de CK. Para los materiales compuestos con incorporación de EP y RB en 4%, reportaron resistencia a la compresión de 32 y 45 MPa a 28 días, y densidades de 1853 y 1922 kg/m^3 respectivamente, lo cual representa una reducción de 6,08% y 2,58% en comparación a la matriz de referencia. La conductividad térmica de los compuestos con 4% de EP y RB fue de 0,314 y 0,344 W/m.K, y el coeficiente de absorción acústica a frecuencia de 500 Hz fue de 0,7 y 0,5 respectivamente. Las propiedades de desempeño evaluadas mostraron la facilidad de usar 4% de EP y RB para la manufactura de materiales compuestos para aplicaciones como paneles de aislamiento térmico y acústico.

Palabras clave: *aislamiento termoacústico, geopolímero, madera, poliestireno expandido, residuos de caucho.*

1. Introduction

Lightweight Portland cement concretes have been gaining a position in the last decade due to their functional advantages such as a greater capacity for thermal and acoustic insulation, and low density, notable advantages compared to conventional concrete [1–3] In concrete-based constructions, the self-weight of the structure represents a significant proportion of the total load, using concrete with a lower density would reduce dead loads, and allowing faster construction system, and low costs due to transport. These materials can be produced by incorporating lightweight aggregates or air bubbles into the cementitious matrix.

Traditionally expanded clays such as perlite or vermiculite have been used for the production of lightweight concrete, however, the use of these involves high energy consumption, because high temperatures are required in their production process [4,5] Other alternative materials have been investigated to providing better living comfort, allow reducing the environmental impact generated by the use of traditional materials [6–8].

The alternative materials including corkwood particles (CK), tire rubber waste (RB), and expanded polystyrene (EP) waste have been used as aggregates for concrete because they provide good acoustic insulation properties [6,9]. Corkwood chipboard has a noise reduction coefficient (NRC) of 0.4, expanded polystyrene and recycled rubber chipboard a NRC of 0.5, and the traditionally used polyurethane of 0.68 [10]. In this sense, [11] evaluated the effect of polystyrene foams on Portland cement concretes obtaining concretes with low density (150–170 kg/m^3) and low thermal conductivity (0.06–0.064 W/mK).

Corkwood has been used in the manufacture of expanded agglomerated composites, which have been molded at a temperature between 250-300 °C with pressure, allowing the obtaining of panels and plates with the potential to be used in rail transport [12]. Tire rubber waste is a material that, due to its low compressibility and large volume, presents problems to be deposited, these materials have traditionally been used in the manufacture of asphalt mixtures and Portland cement mixtures [13]. Followed, [14] evaluated the properties of lightweight Portland cement mortars using EP particles (0.8% and 1.6%) used as a coating on walls and ceilings; although they observed reductions in compressive strength, the values were in the range specified for covering mortars (5 and 13 MPa), and additionally, the thermal conductivity decreased by 47% compared to a commercial mixture.

In Colombia, during the years 2013 - 2017, around 6.500.000 tons of tire wastes were collected from 177 collection sites located in different cities [15]. In the case of EP, in the United States, it is reported that the recycling capacity is around 28%, while in Colombia the recycling of EP is minimal, it does not go beyond initiatives and research from different universities [16], although the government has legislated through the [17], to reduce the production and consumption of single-use plastic to the minimum possible in the national territory.

On the other hand, due to the increase in the popularity of the use of ecological construction materials, with a lower carbon footprint and, if possible, have a low cost, in the construction industry, alternative materials to traditional Portland cement have emerged, among these are alkaline activation materials and so-called geopolymers. This is produced from a process of polymerization of raw materials with a high content of SiO_2 and Al_2O_3 in presence of alkaline solutions, where most of the aluminosilicates used are minerals and different industrial waste [18–20].

Geopolymers are considered as materials that can replace Portland cement in some applications and their advantages include obtaining at low temperatures, acceptable compressive strength at short curing ages, good chemical and high temperatures resistances, as well as potential reduction of CO_2 emissions [7,19,21–26]. However, there are few studies on the use of geopolymer paste that may have potential applications as construction materials with thermal and acoustic insulation capacity.

In this regard, the following have been studied: (i) the use of foaming agents such as H_2O_2 and aluminum powder to generate air bubbles within the metakaolin-based geopolymer paste, reaching compressive strengths of between 0.6 -14.5 MPa and density between 600-1000 kg/m³ [27,28] Silica fume for the generation of foams and their

performance at high temperatures has also been investigated [26]. Aluminum powder was studied in obtaining foamed materials with pore volume between 30-70% obtaining thermal conductivities between 0.15-0.4 W/mK [29]. In foamed geopolymers based on alkaline activation of fly ash, compressive strengths of up to 6.76 MPa have been reported and it has been found that when the foams are exposed to high temperature they can form crystalline phases such as anorthite and mullite [30]. The use of lightweight particles such as expanded vermiculite in geopolymer paste has made it possible to obtain composite materials with density in the range of 700 - 900 Kg/m³, with average strength of 2 MPa and thermal conductivity of 0.2 W/mK [31].

Wood particles have been used for the production of geopolymer composites based on fly ash/metakaolin [32], which have reported density between 700-350 Kg/m³ and porosity between 10-28% in samples cured at room temperature when the wood content varies between 10 – 60 wt%; for these composites, the compressive strength reached ~2 MPa with 60wt% of wood particles in geopolymers cured at room temperature and ~ 6 MPa in geopolymers cured at 80 ° C for 24 hours. The pinewood has also been investigated, finding that depending on the composition, the thermal conductivity of 0.088 W/mK is reached in materials with compressive strength of 2.84 MPa and flexural strength of 1.5 MPa [33]. The workability in geopolymer composites with wood particles is reduced due to the greater demand for activators such as NaOH and sodium silicate [32].

Geopolymer composite materials with pumice stone particles and 2.5wt% aluminum powder have reached density of 0.9 g/cm³ and compressive strength of 1.6 MPa at 28 days, after thermal curing at 40°C [34]. EP particles have also been used to produce lightweight geopolymers, [35] found that geopolymers based on fly ash with 3wt% EP had low thermal conductivity (0.16

W/mK) and density of 0.5 g/cm^3 with 11 MPa compressive strength. [8] produced geopolymer from the activation of metakaolin with marble dust as a source of CaO using solutions of sodium silicate + NaOH and 72.5wt% EP waste particles; the authors report a thermal conductivity of 0.121 W/mK, density between 500-550 kg/m^3, compressive strength between 1.8-2.5 MPa and flexural strength between 0.20-0.35 MPa. [7] successfully prepared lightweight geopolymer panels from the alkaline activation of metakaolin with sodium silicates + NaOH, incorporating H$_2$O$_2$ and EP particles. When the mass ratio of metakaolin/EP particles was 1:1, they obtained compressive strength of up to 3.0 MPa and thermal conductivity ~ 0.035 W/mK with 100 kg/m^3 density. [36] studied the use of EP particles in the manufacture of lightweight concrete based on the fly ash alkali activation, suggesting the use of the materials in insulation applications.

This research evaluates the use of expanded polystyrene (EP), tire rubber (RB), and corkwood (CK) particles wastes in the design of geopolymer-based composites using metakaolin as the aluminosilicate precursor, with the objective of manufacture a material with thermo-acoustic properties. The effect of the incorporation of different particles in compressive strength, density, absorption, porosity, thermal conductivity, acoustic insulation, and microstructure of the composite material was evaluated.

2. Methodology

2.1 Raw materials

The aluminosilicate source for geopolymer paste is a commercial metakaolin (MkF). The chemical composition of MkF is shown in Table 1, and it was determined by X-ray fluorescence (XRF) using an AXIOS mAX spectrometer (PANalytical, USA), with 4.0 KW maximum power. The SiO$_2$/Al$_2$O$_3$ molar ratio for MkF was

2.20. The MkF was mineralogically characterized by XRD using an X'Pert MRD PANalytical diffractometer with CuKα radiation generated at 20 mA and 40 kV. The specimens were scanned between 10° and 60° 2θ, with a step size of 0.02° at a speed of 4.0 s per step. The results for XRD are shown in Figure 1.

A slight baseline uplift between 20°-30° 2ɵ indicates the content of material an amorphous state, although, it was identified high content crystal phases as quartz (SiO$_2$, Inorganic Crystal Structure Database 079634) and residual kaolinite (Ref. code 001-0527). The quartz content is a common impurity for Colombian kaolin and does not is removed during thermal treatment of these [37,38] probably due a short residence time of the kaolin in the kiln [39]. The particle size distribution was determined using a laser particle size analyzer (Mastersizer 2000, Malvern, UK). The particle average size was 17.2 μm. The MkF density is 2550 kg/m^3 and was calculated according to the pycnometer method (ASTM C329).

EP, RB and CK particles were selected to produce geopolymer-based composite. The EP, RB, and CK particles had a density of 27.5, 950, and 650 kg/m^3 respectively, and were determined by Archimedes Method. The particle average size for EP and RB was 2.35 mm. The corkwood was mechanically conditioned by mixer for 5 minutes until achieve 2.3 mm particle average size. The alkali activator used to produce de geopolymer was a mix of sodium silicate (32.24wt% SiO$_2$, 11.18wt% Na$_2$O y 55.85wt% H$_2$O) and industrial sodium hydroxide (NaOH). The solution modulus was 2.97.

2.2 Design and preparation of geopolymer

The parameters to produce geopolymer paste were obtained by modifying variables from previous studies published by [40] and [41,42]. Two dosages were evaluated, which are shown in Table 2.

Table 1. *Chemical composition for MkF.*

	Compound (wt%)									
	SiO_2	Al_2O_3	Fe_2O_3	CaO	MgO	Na_2O	K_2O	SO_3	TiO_2	L.O.I*
MkF	52.67	40.63	1.35	0.53	0.31	0.07	0.56	0.05	1.08	2.61

*L.O.I: loss on ignition. Source: own elaboration
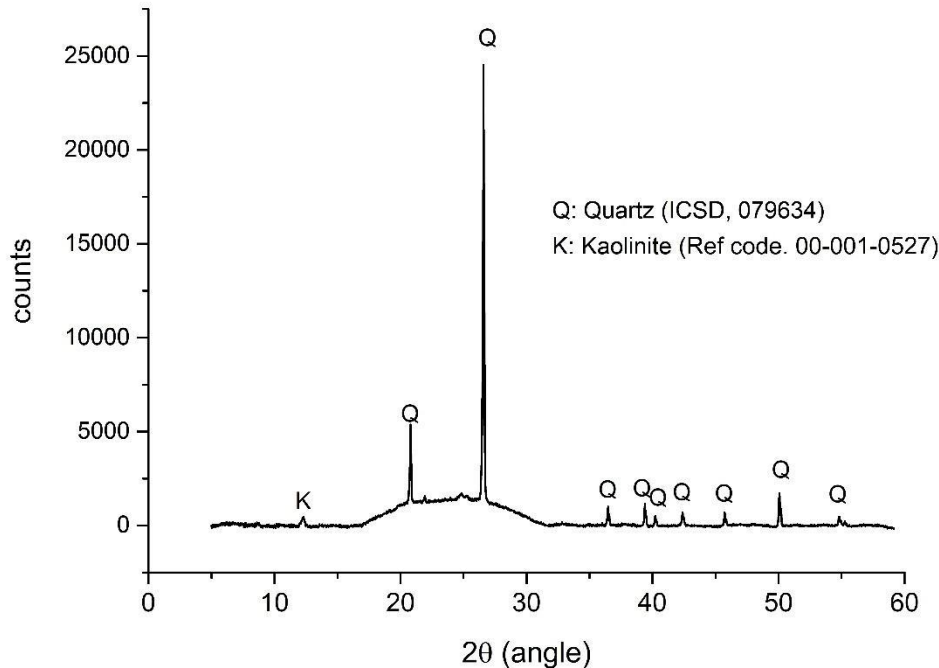
Figure 1. *X-Ray diffraction patter of the MkF. Source: own elaboratorion*

The liquid/solid ratio was 0.4. The mixing procedure to obtain the geopolymer reference is as follows: i) dissolution of the NaOH particles in water by stirring for 10 minutes to guarantee their complete dissolution, ii) mix with the sodium silicate and rest the solution for 30 minutes; iii) mixing the activating solution with MkF for 7 minutes in a Hobart mixer.

The liquid/solid ratio used for manufacturing composite materials was adjusted to 0.49 to achieve adequate workability of the mixtures with particle incorporation. For manufacturing of composite materials, the EP, RB, and CW particles were incorporated in percentages of 2, 4, and 6% by volume, and mixing was continued for 2 more minutes. Subsequently, the materials were poured into 2" x 2" x 2" molds and wrapped with a plastic polyethylene film to avoid rapid evaporation of the water. Finally, they were placed in a chamber at room temperature of 25 °C ± 2 °C and relative humidity of 90% until the test age. In order to improve the adherence of the geopolymer with the EP particles, a surface treatment with ethyl-vinyl acetate (EVA) was carried out. This treatment consisted of immersing the EP particles in a 3:1 mixture of water and EVA for a time of 5 minutes until they were completely impregnated and then mixing with geopolymer paste.

Table 2. *Mixing ratios*

Sample	SiO$_2$/Al$_2$O$_3$ molar ratio	Na$_2$O/SiO$_{2 \text{ molar}}$ ratio
GP2.5	2.5	0.25
GP2.8	2.8	0.28

Source: own elaboration

2.3. Characterization of paste and geopolymer composite

The following techniques were used:

- The geopolymer pastes were characterized as KBr pellets by Fourier transform infrared (FTIR) spectroscopy on a PerkinElmer Spectrum IR 100 spectrometer was used in transmittance mode. The spectra were collected at a room temperature of 25°C, over a wavenumber range of 4000–450 cm^{-1}.

- Scanning Microscopy Electronic (SEM) was used to evaluate the microstructure of the geopolymer paste. This test was performed with a JEOL, JSM-6490LV instrument using high vacuum (3x10^{-6} Torr); the samples were metalized with gold in a Denton Vacuum Desk IV tank.

- The physical characteristics as apparent density, water absorption, and volume of permeable pores of geopolymer composites were determined according to the methods established in the ASTM C642-13 standard.

- The compressive strength was evaluated at ages of 7, 28, and 90 days using an INSTRON 3369 Universal test machine with a capacity of 50 kN at a deformation rate of 1 mm/min. In each case, three specimens were tested. Cubic samples of 20 mm on the side for the geopolymer paste and 2" geopolymer composites were tested according to the ASTM C109/C109M-10.

- The thermal conductivity was obtained by using a thermal constants Analyzer TP 500 S Hot Disk with a heating power of 956.69 mW

for 40 s, using cubic samples of 20 mm on the side. A C5465 sensor was used.

The acoustic insulation capacity of geopolymer composite was determined with a Sperscientific 850014 sound meter and a frequency emitting source, the frequency range was varied between 100 and 1000 Hz. The experimental setup is shown in Figure 2. An acoustic chamber was manufactured by joining five plates (30 mm thick). The dimensions of the side plates were 320 x 80 mm, and the front and back plates were 80 x 80 mm. The plates were manufactured in each case using the materials to be evaluated (paste and geopolymer composite selected). The test consisted of measuring maximum and minimum points for each frequency evaluated during a time of 5 minutes. Two conditions were evaluated: normal noise conditions outside of the boxes, and inside them to evaluate the amount of sound transmitted through the developed material.

3. Results

3.1 Initial stage: selection of geopolymer paste

The compressive strength of geopolymer pastes is shown in Figure 3. At different curing ages evaluated, the GP2.8 geopolymer shows a higher strength in comparison to the GP2.5 geopolymer. From day 1 until day 90, the increase in compression strength was 68.24% and 56.83% for GP2.5 and GP2.8 respectively, with strength at 28 days of 8.55 MPa (GP2.5) and 25.96 MPa (GP2.8).

It is expected since a higher Na$_2$O/SiO$_2$ ratio generates a greater dissolution of metakaolin and because it contains a greater amount of active silica (higher SiO$_2$/Al$_2$O$_3$ ratio for GP2.8). A greater poly-condensation and increased reaction products are produced, specifically, hydrated aluminosilicate gel (N-A-S-H) [40,43]. This effect can be corroborated with FTIR spectra (Figure 4), the shift of principal band (~1003 cm^{-1} to GP2.5) to smaller wavelength (999 cm^{-1} to GP2.8) are
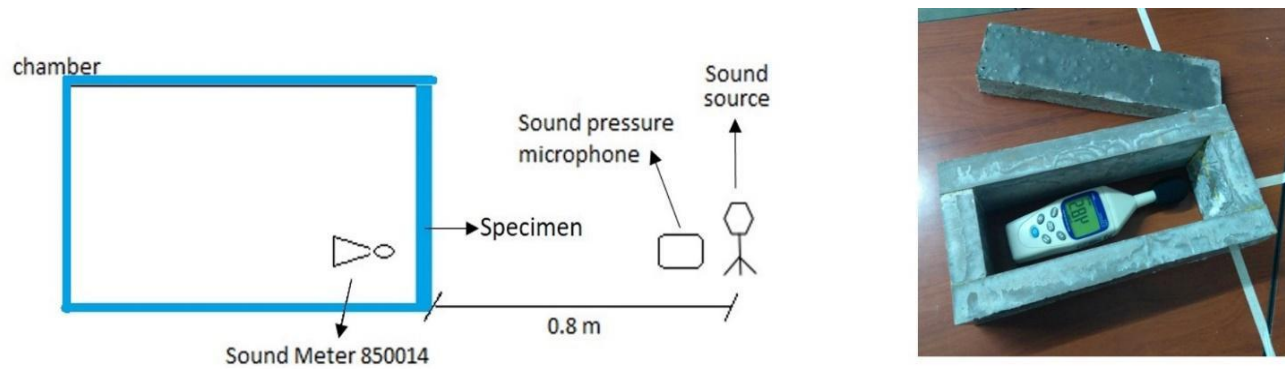
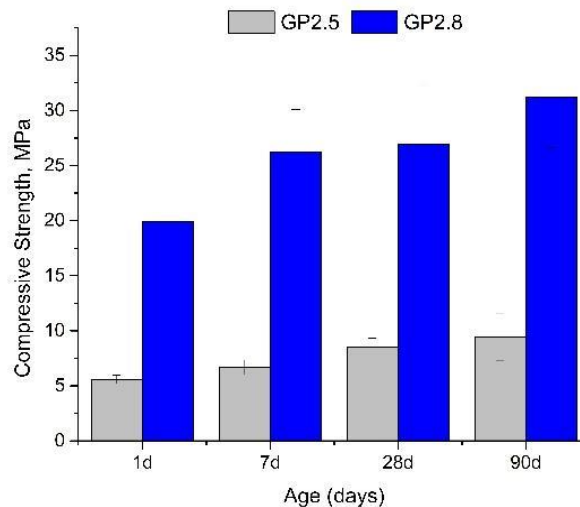**Figure 2.** *Experimental setup used for measurement of acoustic properties. Source: own elaboration*

Figure 3. *Compressive strength for geopolymer pastes GP2.5 and GP2.8. Source: own elaboration*

attributed to the development of higher quantities of amorphous structures where silicate species are partially substituted by aluminate species [41, 43].

In Figure 4 is shown the FTIR results for alkali-activated pastes GP2.5 and GP2.8 at different curing days (1, 7, and 28 days) in comparison with MkF raw material. For MkF there is an absence of hydroxyl stretching bands, meanwhile, in alkaline activated samples (GP2.5 and GP2.8) it is possible to find a wide band located between 3445 - 3465 cm^{-1} which is attributed to the stretching vibration of the H-OH groups [44], while the band located at ~1660 cm^{-1} is associated to the

stretching vibration of the H-OH groups associated to the reaction products as N-A-S-H, the weak H_2O molecules that are trapped in the cavities of the structure [45]. For MkF the band at 814 cm^{-1} can be assigned to Al^{IV}–O and the band at 1089 cm^{-1} is Si-O stretching band [38].

To GP2.5 and GP2.8, the presence of a wide absorption band, between 1003 and 999 cm^{-1} is associated with the asymmetric stretching vibrations of the Si-O-Si and Si-O-Al bonds of the TO$_4$ tetrahedral (T=Si or Al), [46,47]. At the age of 1 and 7 days, this band is centered at wavelengths of 1003 cm^{-1}. At 28 days, in the case of GP2.8

geopolymer paste this band shifts to lower wavelengths (999 cm⁻¹), which may be associated with a higher dissolution of MkF and the occurrence of more polycondensation reactions to give rise to an aluminosilicate structure where

silicate species are partially replaced by aluminate species [42,43,48]. This confirms the better compressive strength results shown in the GP2.8 paste compared to GP2.5 (Figure 3).
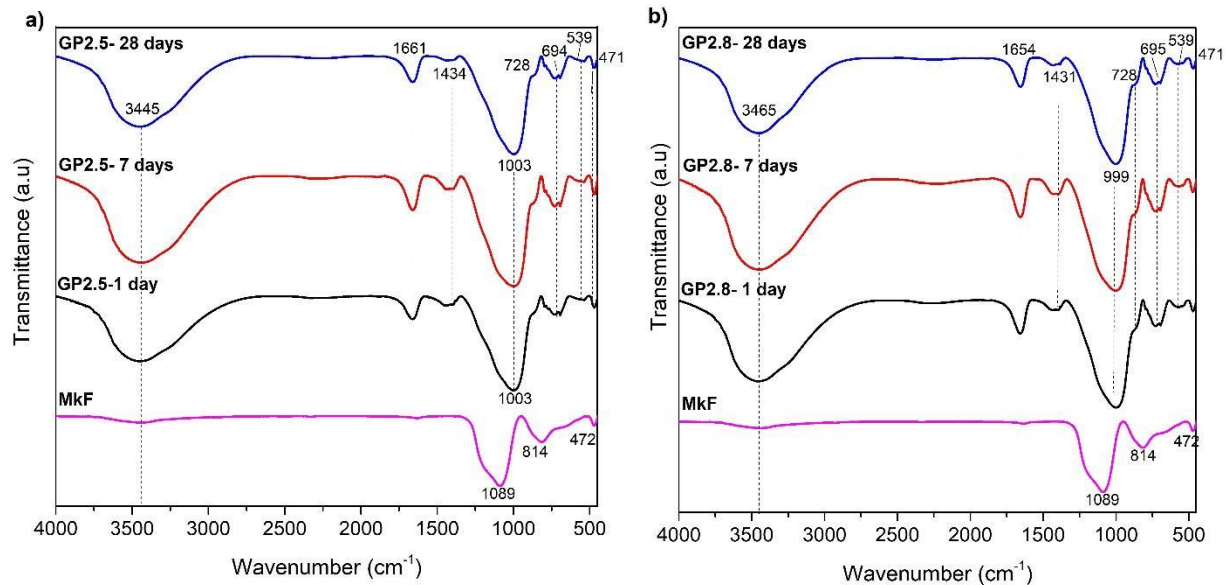

Figure 4. *FTIR for (**a**) Geopolymer pastes (**b**) MkF raw material. Source: own elaboration*

The small peak centered at 728 cm⁻¹ indicates bending vibration of Si-O-Al bonds, this band is characteristic of geopolymer materials and is generated after the reaction between silicon aluminates and the highly alkaline solution [45]. [49] affirm that the formation of this band is associated with the formation of a highly cross-linked geopolymer gel. The bands centered at ~1434 cm⁻¹ represent the -CO-type bonds corresponding to the vibrations of CO_3^{-2} compounds, in particular to the formation of alkaline carbonates, Na_2CO_3 [50,51] generated by the reaction of the Na^+ rich pore solution with the CO_2 in the atmosphere [42,44,52]. The bending vibration signals of the Si-O-Si link are at 471 cm⁻¹, and the signals detected at wavenumbers between 538-543 cm⁻¹ are associated with the symmetrical deformation of the Si-O-Al links [45,53].

The GP2.8 paste was chosen according to these initial results in the choice of the geopolymer paste, for the manufacture of the particulate geopolymer composites with the incorporation of EP, RB, and CK, which for purposes of comparison with the composite materials, will be identified from now on as GP.

3.2 Geopolymer composites

3.2.1. Physical properties: Density, porosity, and absorption.

Figure 5a shows the results of density and water absorption for the different materials developed. The apparent density of the reference GP was 1973 kg/m³, and the dry density was 1530 kg/m³. The incorporation of EP, RB, and CK particles, in general, decreases the density in tecomposite materials by the proportion of particles added to

the mixture, which is following what is expressed by other authors [54]. Comparing the EP, RB, CK-based composites, the lowest density is obtained with the incorporation of EP particles whose nominal density (27.5 kg/m^3) is the lowest of the three particles used. In the case of E-based composites, the density of the materials decreases significantly as the percentage of EP increases, up to 7.7% for EP6. Although the study of [7], introduced greater amounts of EP achieving that the composite had tendency to float in the water, the trend observed in this study is maintained.

By using the RB particles, the density of the composites was decreased between $2.28 - 3.09\%$. In the case of composite materials with CK particles, the reduction in density was less than 2%.

The water absorption for the RB4, RB6, EP4, and EP6 composites decreased compared to the GP paste by 14.43%, 17.25%, 45.07%, and 55.28% respectively. The high-water absorption in the GP paste is associated with a paste with a high content of micro-cracks, micro-porosities, and unreacted MkF amounts (SEM results). The use of CW particles produced the most permeable composite materials, while the most significant decrease in the absorption was obtained with the EP particles due to its hydrophobic character; these can be considered as a closed-cell foam constituted essentially with 98% of air [55]; these results coincide with the reported by [7]. [35] reports in mortars manufactured with EP a water absorption of up to 11.8%; and in the present investigation, the composite materials EP2 and EP6 reported water absorption values of 10.42% and 6.87%, respectively. These values are comparable to the absorption reported for Portland cement-based mortars, whose value fluctuates between 6 and 13%, depending on the material compressive strength [13].

Comparing the results of open porosity (Figure 5b) for geopolymer composites with the GP paste, it was found that the lesser affectation is for

samples with the incorporation of CW particles, decreases of up to 7.18% for W4 was found. This behavior is attributed to the highly porous and connected cellular structure of CK, with high contents of lignin (22%) and suberin (40%), and at the same time to the highly hygroscopic character. [55] found that cork particles retain large amounts of water, which increases the weight of the particles by 400%, being released after 1 h. Therefore, in the case of the geopolymer composites in this study, it is believed that the CK particles absorbed part of the alkaline solution and this generated the subsequent deterioration of the particles. It is clarified that no treatment was made to the cork particles before their incorporation for the manufacture of geopolymer composites. On the contrary, in the composite materials with EP, a reduction in porosity between 29.54 and 55.25% compared to the GP paste is observed, and in the RB-based composites, porosity decreased between 14.52 and 16.9%. The porosity results obtained in this study are lower than the values reported for OPC cement mortars added with RB [13].

3.2.2. Mechanical properties for geopolymer composites

The compressive strength results of geopolymer composites, prepared with different content of RB, EP, and CK particles, are shown in Figure 6. In general, it was found that the incorporation of particles decreases the compressive strength of geopolymer compared to the unreinforced GP paste.

Thus, for the RB2, RB4, and RB6 composites the losses in compressive strength at the age of 28 days were 17.22, 13.70, and 20.19% respectively. Similar results have been reported by [56] when using Portland cement paste. It should be noted, that the adhesion of RB rubber particles to the geopolymer paste is poor, which caused them to detach easily during the compression test, as can be seen in Figure 7a; similar results were found by [57] and [58] using Portland cement binders.
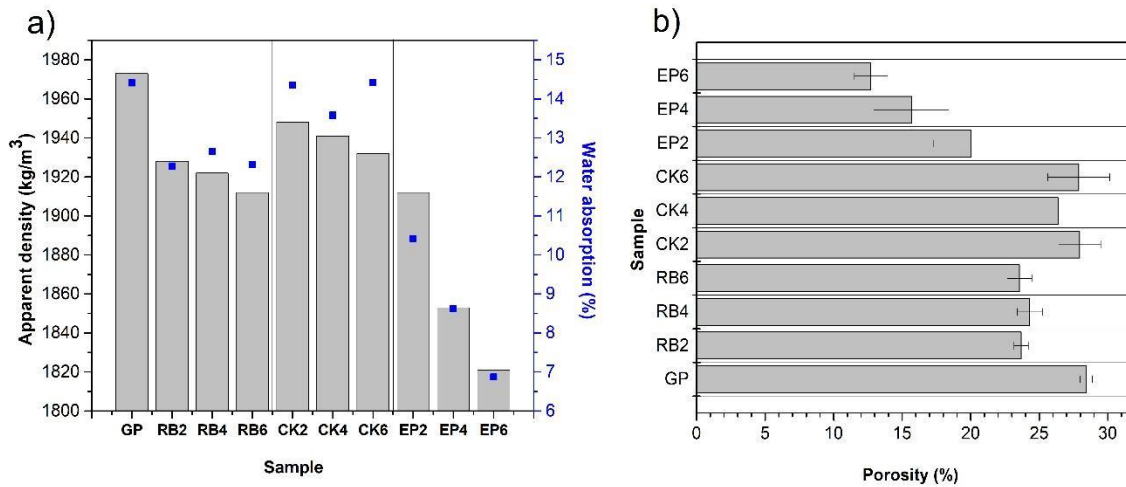
Figure 5. *Physical properties for geopolymer composites compared with GP paste. **(a)** Density vs water absorption and **(b)** Open porosity for geopolymer composites. Source: own elaboration*

For composite materials with EP and CK particles, in general, as the particle content increases, the strength decreases, and this effect becomes more significant with advancing curing age. At 7 days, the compressive strength for CK2, CK4, and CK6 were 45, 42, 40 MPa respectively, however, at 28 days was a drastic strength drop of up to 72.5% (CK6). For CK composites, this behavior can be attributed to the low rigidity, low strength, and large compressive deformations of the CK particles, factors that directly affect the mechanical performance of the composite material [59]. Additionally, the deterioration of the strength of cork-based composites could be by alkaline attacks on the particles (Figure 7b), specifically on the lignin component which is characterized by presenting a low resistance to strong alkalis, such as NaOH [55].

For EP-based composites, this can be attributed to factor as the low strength and high compressibility of EP particles, the poor transition zone between the EP particle and the GP paste (Figure 7c), and the formation of microcracks in this area as evidenced by the SEM results. This behavior has been previously identified by Sayadi

[60] and Duan [7]. Nevertheless, the mechanical performance achieved in this research in EP-based composites is higher than those reported by other authors as [7] who replacing 25wt% GP by EP particles and report 4 MPa; and [61] who achieved 3 MPa to ultra-low density geopolymer composites with 25wt%-vitrified microspheres.

In addition, the smooth surface of the EP particles and the poor interfacial bonding (as shown in Figure 7c), its non-absorbent hydrophobic characteristic (although EVA was used to improve the adherence of the particles to the geopolymer paste), result in a failure mode that occurs in the transition zone for lower stress values than those reported for the geopolymer paste, generating detachment of the EP particles; similar results have been found by Tamut when using EP in Portland concrete [62]. At 28 days, the behavior is more drastic, due to the poor bonding and higher autogenous shrinkage that occurs in the hardened geopolymer paste. [35] found that increases of the EP particles up to 3 wt% decreases the geopolymer density by 40% and the strength reaches 10 MPa with densities close to $500 \, kg/m^3$. In this research, for the percentages of.
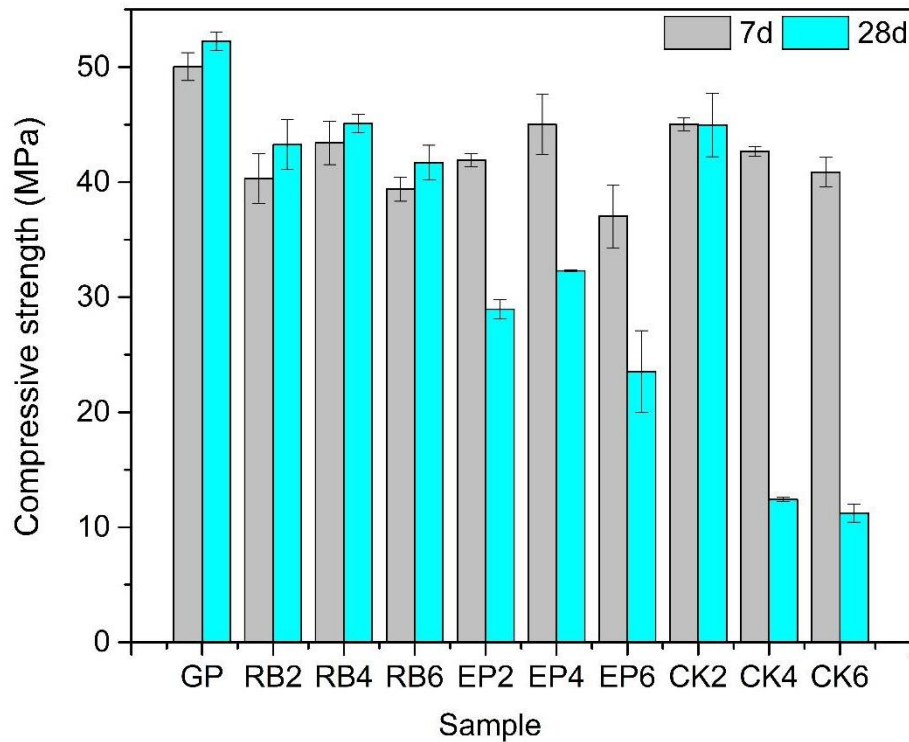
Figure 6. *Compressive strength for geopolymer composites at 7 and 28 curing days. Source: own elaboration*

Figure 7. *Optical microscopy images in stereoscope for geopolymer composites at 28 curing days: (**a**) RB2, (**b**) CK4 (**c**) EP2. Source: own elaboration*

EP studied, the compressive strength is between 22-30 MPa after 28 days of curing. [14] used EP particles in 0.8% and 1.6%, reports compressive strengths between 5 and 13 MPa suggesting the use of these materials as coating mortars. The SEM images of the geopolymer paste (GP) and composite materials with 2% RB and EP particles at 28 days are shown in Figure 8. In the GP paste (Figure 8a) the presence of unreacted MK particles embedded in the geopolymer gel (N-A-S-H) can be seen, as well as a porous surface and

presence of microcracks which correlates with the highest water absorption previously reported; this microstructure is typical of metakaolin-based geopolymers [7]. To 2%EP-based composites (Figure 8b) and 2% RB (Figure 8c), it was possible to measure the interface zone between the paste and the reinforcement. In the compound with EP, the interface is 47.11 μm wide and several microcracks are evidently growing from the EP-geopolymer interface, which is an indication of the low compatibility between the
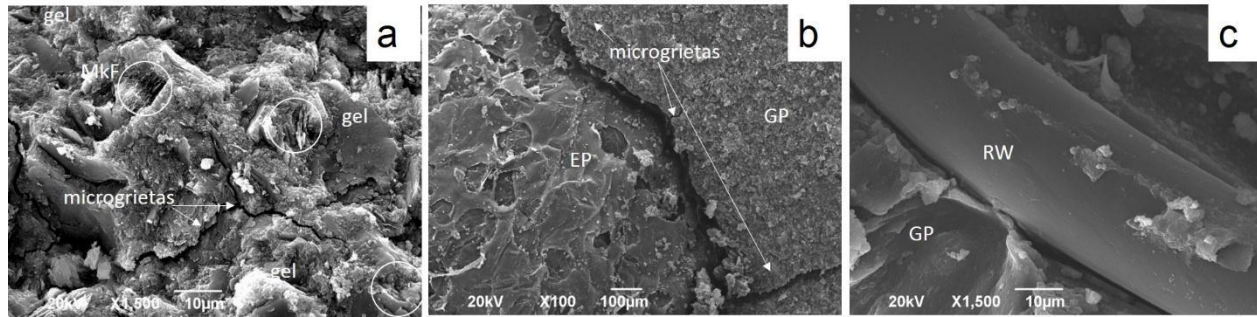
Figure 8. *SEM images at 28 curing days for geopolymer (**a**) GP paste, (**b**) EP2 composite (**c**) RB2 composite.*
Source: own elaboration

EP particles and the geopolymer paste and explains the decay of the compressive strength for these composites after 28 days of curing. In RB-based composites, the interface is 1.31 μm wide, and it was also observed that the RB particles are not spherical, they have a fiber shape and as reported by [63] the morphological characteristics influence the mechanical results. In RB2 composite (Figure 8c), no microcracks are observed, which would explain the best results obtained in the compressive strength test.

3.2.3. Thermo-acoustic properties

From the previous results, the composite materials RB4 and EP4 were selected to evaluate the thermal conductivity and the acoustic insulation capacity and to compare these with those obtained in the GP paste.

Thermal conductivity

Figure 9 compares the thermal conductivity and pore volume of the GP paste and the EP4 and RB4 composites. A lower porosity and thermal conductivity can be seen in the composite materials. The thermal conductivity of the GP paste (0.48 W/mK) was reduced by 34% when EP was incorporated, which is attributed to the low density of the EP particles (27.5 kg/m^3) as they are essentially constituted of polymer chains with 98% of encapsulated air. [14], in OPC mortars lightened with EP (0.8 and 1.6%) reports a

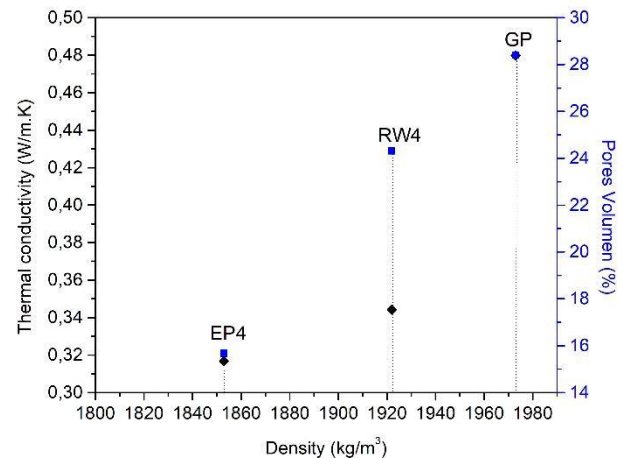decrease of up to 47% in thermal conductivity, obtaining values between 0.42 and 0.33 W/mK.

Figure 9. *Thermal conductivity vs pore volumen for GP paste, EP4 and RB4 composites. Source: own elaboration*

These results are similar to those reported for geopolymer composites in this study. However, other authors such as Brás [55], for OPC mortars added with EP particles report thermal conductivities between 1.2 - 1.4 W/mK for materials with densities between 1850-1950 kg/m^3, contrasting with what is reported by [64], who with the incorporation of 3 wt% EP managed to produce geopolymer concrete with conductivities of 0.16 W/mK, density of 1100 kg/m^3 and 11 MPa of compressive strength. For RB4 composite, thermal conductivity decreased by 28% with respect to GP paste conductivity;

similar results, 0.33 and 0.38 W/mK were found in OPC composites by Cintra [4] when incorporating 10 and 33% in weight of RB respectively.

Acoustic Behavior

Fibrous materials, cellular materials, organic materials, and natural materials such as pumice and some woods are known to possess acoustic insulation properties [65]. High porosity and low density are characteristics considered necessary to obtain good acoustic absorption behavior and to reduce the transmission time at medium and high frequencies or to increase the acoustic insulation of walls in buildings [66]. In general, a good sound absorption material has sound absorption coefficients close to 1 over a wide range of frequencies [13,65].

Figure 10 shows the results of the sound energy transmission and the sound absorption coefficient for the EP4 and RB4 composites and the GP paste in the frequency range of 100 - 1000 Hz. The measurement of the sound transmission is based on the ratio between the sound wave transmitted on the rear surface and an incident sound wave on the front surface of acoustically absorbent and porous material. As the sound wave travels, the differences in the cross-section of the material dampen the sound wave and therefore reduces the intensity of the transmitted sound. The loss of sound transmission also represents the characteristic damping properties of the material, a high value results in more sound that can be attenuated [67]. The geopolymer composites developed here have a loss in sound energy transmission ~51% for frequencies of 100 Hz when compared to the GP paste, which can be categorized as acoustic isolators.

The human ear picks up sound intensity levels between 0 dB (threshold) and 120-130 dB. This is true for the mid-frequency range (1000-2000 Hz). For lower or higher frequencies, the dynamics are reduced. However, all sounds above 90 dB damage the inner ear and can even cause irreversible damage above 120 dB [68]. In the case of the GP geopolymer paste, the energy transmitted for frequencies between 100-100 Hz is between 25-35 dB, this material presents a higher sound transmission in comparison to the composite materials evaluated because its microstructure is much more compact and being the denser material, it favors the transmission of waves within it.

However, it should be noted that the acoustic properties depend on the frequency at which they are measured [66]. The EP4 and RB4 composites could be classified as acoustic insulation materials, since according to [10] within this classification are those materials that present an acoustic energy transmission lower than 30 - 40 dB, and as it can be seen in Figure 10a, for the EP4 and RB4 composites the transmitted energy is lower than 20 dB for frequencies between 100-1000 Hz.

In this sense, [13] manufactured OPC mortars incorporating RB rubber particles and reported that for frequencies of 400-2500 Hz the sound absorption coefficients are between 0.1-0.2 when incorporating 10.15 and 20% RB; the test was conducted using the impedance tube method. One factor that affects acoustic performance is particle size, in this respect [69] report for RB that the larger the particle size the higher the sound absorption coefficient, so for particles of sizes between 1 - 3 mm (as used in this study) the absorption coefficients obtained are in the range of 0.8-0.15 when replacing, in OPC concrete plates, sand by percentages of 7.5% and 15% of RB.

In general, for the whole measured frequency range, more transmission energy is obtained for the GP paste (Figure 10a), and therefore the sound absorption coefficients are higher in geopolymer composites with particles (Figure 10b). This is because, to develop a material that absorbs sound,
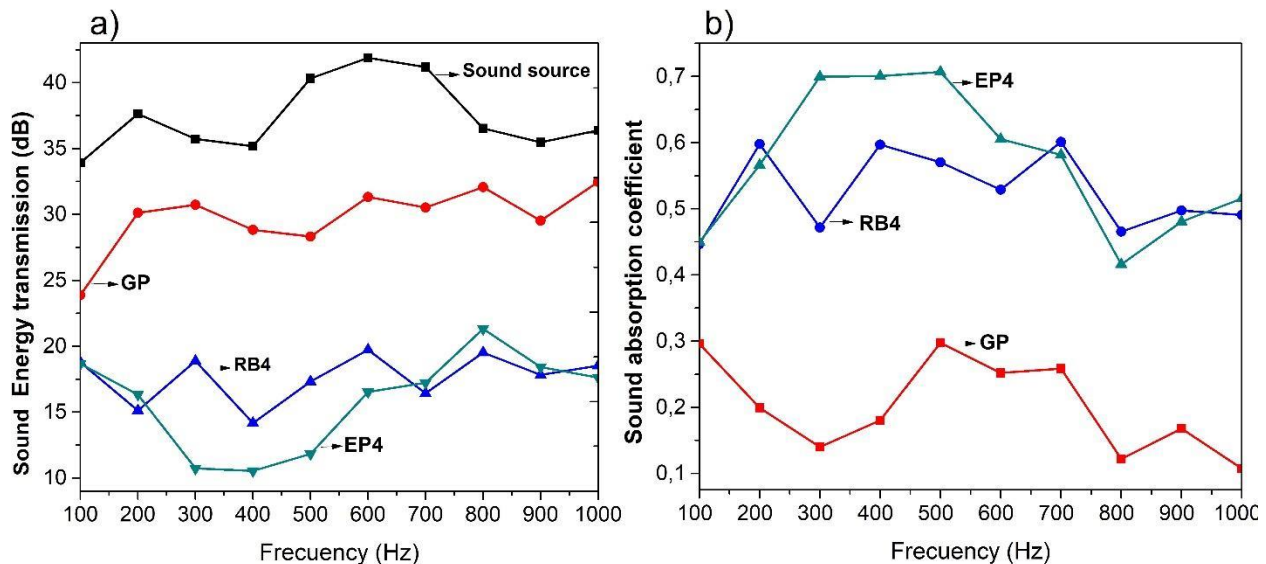
Figure 10. *Acoustic properties for GP, RB4 and EP4 at frequency de 100 – 1000 Hz* ***(a)*** *Energy transmission and* ***(b)*** *Sound absorption coefficient. Source: own elaboration*

it is necessary to create obstacles within the structure where the sound energy can be dissipated. In this study, the obstacles are the RB and EP particles, which as previously determined incorporate large amounts of air within the structure allowing the dissipation of sound waves [70]. For the EP4 composites evaluated in 30mm thick plates, the maximum sound absorption coefficient reached was 0.707 at a frequency of 500 Hz (141% higher than the GP paste), while for the RB4 compound the maximum absorption coefficient was 0.60 at a frequency of 700 Hz (114% higher than the GP paste). It should be noted that some commercial products manufactured with a thickness of 25.4 mm report sound absorption coefficients of 0.77 to 500 Hz [71].

For the same frequency (500 Hz), materials such as rubber waste agglomerate and cork agglomerate present a sound absorption coefficient of 0.8 and 0.42; respectively. Likewise, in standard OPC concretes, absorption coefficients lower than 0.1 have been reported in the low-frequency range (125-2000 Hz) [72]; for which it is evidenced that the geopolymer composites developed here present adequate properties to be considered as acoustic isolators. EP particles also have an absorption coefficient close to 0.42 [10] and in this study values of 0.57 were obtained for the composites with RB4 and 0.70 for EP4 at the same frequency. The acoustic absorption coefficient for composites with the use of EP, in this research the improvement for a frequency of 500 Hz was 141% in the EP4 composite.

4. Conclusions

Geopolymer composites developed have an environmental impact considered low, thanks to the incorporation of particles from tire waste. Additionally, the composites with the incorporation of 4% of EP and RB particles present a compressive strength of 32 and 45 MPa. The composite materials reached an apparent

density of 1922 and 1853 kg/m^3 achieving a reduction of 2.58% and 6.08% for RB4 and EP4 respectively compared to GP paste.

It was found that the inclusion of EP and RB particles decreases the water absorption in the developed materials, because the particles are hydrophobic and replace the volume previously occupied by a highly permeable GP paste.

The EP4 and RB4 composites have a low thermal conductivity (0.316 and 0.344 W/mK), which could give them the opportunity in the manufacture of panels in the construction industry, also is highlights the low sound absorption coefficients achieved for frequencies of 500 Hz of 0.70 and 0.50 for EP4 and RB4 respectively.

The high alkalinity of the GP paste caused a deterioration of the CK particles, and these composites were discharged.

5. Funding Statement

6. References

(1)   Karlsson KF, TomasÅström B. Manufacturing and applications of structural sandwich components. Compos Part A Appl Sci Manuf. 1997;28(2):97–111. https://doi.org/10.1016/S1359-835X(96)00098-X

(2)   Yang Y, Li B, Chen Z, Sui N, Chen Z, Saeed M-U, et al. Acoustic properties of glass fiber assembly-filled honeycomb sandwich panels. Compos Part B Eng. 2016;96:281-286. https://doi.org/10.1016/j.compositesb.2016.04.046

(3)   Wang L, Chen SS, Tsang DCW, Poon CS, Shih K. Value-added recycling of construction waste wood into noise and thermal insulating cement-bonded particleboards. Constr Build Mater. 2016; 125:316–25. https://doi.org/10.1016/j.conbuildmat.2016.08.053

(4)   Cintra CL, Paiva AE, Dos Santos WN, Baldo JB. Masonry light weight mortars containing vermiculite and rubber crumbs of recycled tires. InterCeram Int Ceram Rev. 2014;63(1–2):40–3. https://doi.org/10.1007/BF03401034.

(5)   Videla C, López M. Efecto de la resistencia intrínseca del árido ligero en la resistencia a compresión y rigidez del hormigón ligero. Mater Constr. 2002;2002(265):23–37. https://doi.org/10.3989/mc.2002.v52.i265.342.

(6)   Asdrubali F. The role of Life Cycle Assessment (LCA) in the design of sustainable buildings: Thermal and sound insulating materials. Edinburg, Scortland: 8th Eur Conf Noise Control 2009, EURONOISE 2009 - Proc Inst Acoust. 2009;31(PART 3).

(7)   Duan P, Song L, Yan C, Ren D, Li Z. Novel thermal insulating and lightweight composites from metakaolin geopolymer and polystyrene particles. Ceram Int. 2017;43:5115–20. https://doi.org/10.1016/j.ceramint.2017.01.025

(8)   Colangelo F, Roviello G, Ricciotti L, Ferrándiz-Mas V, Messina F, Ferone C, et al. Mechanical and thermal properties of lightweight geopolymer composites. Cem Concr Compos. 2018;86:266–72.

https://doi.org/10.1016/j.cemconcomp.2017.11.016

(9) Dissanayake DMKW, Jayasinghe C, Jayasinghe MTR. A comparative embodied energy analysis of a house with recycled expanded polystyrene (EPS) based foam concrete wall panels. Energy Build.2017;135:85–94. https://doi.org/10.1016/j.enbuild.2016.11.044.

(10) Pedroso M, Brito J De, Silvestre JD. Characterization of eco-efficient acoustic insulation materials (traditional and innovative). Constr Build Mater. 2017;140:221–8. http://dx.doi.org/10.1016/j.conbuildmat.2017.02.132

(11) Laukaitis A, Žurauskas R, Kerien J. The effect of foam polystyrene granules on cement composite properties. Cem Concr Compos. 2005;27(1):41–7. https://doi.org/10.1016/j.cemconcomp.2003.09.004

(12) AI A group. Construction - Acoustic Insulations. AMORIM. Cork Composites. 2019. Available from:https://amorimcorkcomposites.com/en/search/?q=acoustic%20insulation&tag=acoustic%20insulation

(13) Corredor-Bedoya AC, Zoppi RA, Serpa Al. Composites of scrap tire rubber particles and adhesive mortar – Noise insulation potential. Cem Concr Compos. 2017;82:45–66. https://doi.org/10.1016/j.cemconcomp.2017.05.007

(14) Herrera Góngora M. Propiedades mecánicas, térmicas y acústicas de un mortero aligerado con partículas de poliestireno expandido (EPS) de reciclaje para recubrimientos en muros y techos [Tesis de Maestría]. Centro de Investigación Científica de Yucatán, A.C. Centro de Investigación Científica de Yucatán, A.C.; 2015. Available from: https://cicy.repositorioinstitucional.mx/jspui/handle/1003/413

(15) Medio Ambiente. Para las llantas usadas sí hay una vida después de la muerte. Dinero Magazin. Revista Dinero [Internet]. Bogotá. Septiembre 9 de 2017. Available from: https://www.dinero.com/pais/articulo/reciclaje-de-llantas-usadas-en-colombia/249688

(16) Agudelo A, Vega A., Rodríguez, JDJ, Varela JS, Benavides A. Re-diseño de un proceso que permita el reciclaje del poliestireno expandido EPS. Cali: Pontificia Universidad Javeriana; 2017.

(17) Senado de la república de Colombia. Proyecto de Ley No. 050 de 2019 de Senado. Congreso Republica de Colombia 2019 p. 75–84.

(18) Villaquirán-Caicedo MA., Mejía de Gutiérrez R. Synthesis of ceramic materials from ecofriendly geopolymer precursors. Mater Lett. 2018;230:300-304. https://doi.org/10.1016/j.matlet.2018.07.128

(19) Robayo RA, Mejía-Arcila J, Mejía de Gutiérrez R., Martínez E. Life cycle assessment (LCA) of an alkali-activated binary concrete based on natural volcanic pozzolan: A comparative analysis to OPC concrete. Constr Build Mater. 2018;176:103–11.

https://doi.org/10.1016/j.conbuildmat.2018.05.017

(20) Valencia Saavedra WG, Mejía de Gutiérrez R. Performance of geopolymer concrete composed of fly ash after exposure to elevated temperatures. Constr Build Mater. 2017;154:229–35. http://dx.doi.org/10.1016/j.conbuildmat.2017.07.208

(21) Robayo RA, Mejía-Arcila JM, Mejía de Gutiérrez R. Eco-efficient alkali-activated cement based on red clay brick wastes suitable for the manufacturing of building materials. J Clean Prod. 2017;166:242–52. https://doi.org/10.1016/j.jclepro.2017.07.243

(22) Duxson P, Provis JL, Lukey GC, Van Deventer JSJ. The role of inorganic polymer technology in the development of 'green concrete.' Cem Concr Res. 2007;37(12):1590–7. https://doi.org/10.1016/j.cemconres.2007.08.018

(23) Petrillo A, Cioffi R, Ferone C, Colangelo F, Borrelli C. Eco-sustainable Geopolymer Concrete Blocks Production Process. Agric Agric Sci Procedia. 2016;8:408–18. https://doi.org/10.1016/j.aaspro.2016.02.037.

(24) Villaquirán-Caicedo MA, Mejía-de Gutiérrez R. Mechanical and microstructural analysis of geopolymer composites based on metakaolin and recycled silica. J Am Ceram Soc. 2019;102:3653–3662. https://doi.org/10.1111/jace.16208

(25) Abdel Kader MM, Abdel-wehab SM, Helal MA, Hassan HH. Evaluation of thermal insulation and mechanical properties of waste rubber/natural rubber composite. HBRC J. 2012;8(1):69–74. https://doi.org/10.1016/j.hbrcj.2011.11.001

(26) Zhang Z, Provis JL, Reid A, Wang H. Geopolymer foam concrete: An emerging material for sustainable construction. Constr Build Mater. 2014;56:113–27. https://doi.org/10.1016/j.conbuildmat.2014.01.081

(27) Bell JL, Kriven WM. Chapter 10 - Preparation of Ceramic Foams from Metakaolin-Based Geopolymer Gels. In: Lin H, Koumoto K, Kriven WM, Garcia IER, Reimanis IE, Norton DP, editors. Vol. 29, Developments in Strategic Materials: Ceramic Engineering and Science Proceedings. 2009:96-111. https://doi.org/10.1002/9780470456200.ch10.

(28) Natali Murri A, Medri V, Papa E, Laghi L, Mingazzini C, Landi E. Porous Geopolymer Insulating Core from a Metakaolin/Biomass Ash Composite. Environments. 2017; 4(4):86. https://doi.org/10.3390/environments4040086

(29) Kamseu E, Nait-Ali B, Bignozzi MC, Leonelli C, Rossignol S, Smith DS. Bulk composition and microstructure dependence of effective thermal conductivity of porous inorganic polymer cements. J Eur Ceram Soc. 2012;32(8):1593–603. https://doi.org/10.1016/j.jeurceramsoc.2011.12.030

(30) Yang L, Shili Z, Shuhua M, Chunli L, Xiaohui W. Preparation of sintered foamed ceramics derived entirely from coal fly ash. Constr Build Mater. 2018;163:529–38. https://doi.org/10.1016/j.conbuildmat.2017.12.102

(31) Medri V, Papa E, Mazzocchi M, Laghi L, Morganti M, Francisconi J, et al. Production and characterization of lightweight vermiculite/geopolymer-based panels. Mater Des. 2015;85:266–74. https://doi.org/10.1016/j.matdes.2015.06.145

(32) Sarmin SN. Lightweight geopolymer wood composite synthesized from alkali-activated fly ash and metakaolin. Jurnal Teknologi. 2016;78(11):49-55. https://doi.org/10.11113/.v78.8734

(33) Berzins A, Morozovs A, Gross U, Iejavs J. Mechanical properties of wood-geopolymer composite. Eng Rural Dev. 2017;16:1167–73. https://doi.org/10.22616/ERDev2017.16.N251

(34) Çetinkaya S, Kurt H, Kütük N. Lightweight geopolymer made of pumice with various aluminum powder ratios. Acta Phys Pol A. 2017;132(3):544–5. https://doi.org/10.12693/APhysPolA.132.544

(35) Kakali G, Kioupis D, Skaropoulou A, Tsivilis S. Lightweight geopolymer composites as structural elements with improved insulation capacity. MATEC Web Conf. 2018;149:8–11. https://doi.org/10.1051/matecconf/201814901042

(36) Singh B, Gupta M, Chauhan M, Bhattacharyya SK. Lightweight Geopolymer Concrete with EPS Beads. MATEC Web Conf. Central Building Research Institute, India; 2013. https://doi.org/10.1051/matecconf/201814901042

(37) Villaquirán-Caicedo MA, Rodríguez ED, Mejía de Gutiérrez R. Evaluación microestructural de geopolímeros basados en metacaolin y fuentes alternativas de sílice expuestos a temperaturas altas. Ing Investig y Tecnol. 2015;16(1):113–22.

(38) Vizcayno C, de Gutiérrez RM, Castello R, Rodríguez ED, Guerrero CE. Pozzolan obtained by mechanochemical and thermal treatments of kaolin. Appl Clay Sci. 2010;49(4):405–13. https://doi.org/10.1016/j.clay.2009.09.008

(39) Yanguatin H, Tobón J, Ramírez J. Pozzolanic reactivity of kaolin clays, a review. Rev Ing Constr. 2017;32(2):13–24.

(40) Rodríguez ED, Gutiérrez RM de, Bernal SA, Gordillo M. Efecto de los módulos SiO_2/Al_2O_3 y Na_2O/SiO_2 en las propiedades de sistemas geopoliméricos basados en un metacaolín. Rev Fac Ing Univ Antioquia. 2009;(49):30–41. Disponible en :https://revistas.udea.edu.co/index.php/ingenieria/article/view/15884.

(41) Villaquirán-Caicedo MA, Mejía de Gutierrez R, Sulekar S, Davis C, Nino J. Thermal properties of novel binary geopolymers based on metakaolin and

alternative silica sources. Appl Clay Sci. 2015;118:276–82. https://doi.org/10.1016/j.clay.2015.10.005

(42) Villaquirán-Caicedo MA. Studying different silica sources for preparation of alternative waterglass used in preparation of binary geopolymer binders from metakaolin/boiler slag. Constr Build Mater. 2019;227:116621. https://doi.org/10.1016/j.conbuildmat.2019.08.002

(43) Bernal SA, Rodríguez ED, Mejía de Gutierrez R, Provis JL, Delvasto S. Activation of Metakaolin/Slag Blends Using Alkaline Solutions Based on Chemically Modified Silica Fume and Rice Husk Ash. Waste and Biomass Valorization. 2011;3(1):99–108. https://doi.org/10.1007/s12649-011-9093-3

(44) Król M, Minkiewicz J, Mozgawa W. IR spectroscopy studies of zeolites in geopolymeric materials derived from kaolinite. J Mol Struct. 2016;1126:200–6. https://doi.org/10.1016/j.molstruc.2016.02.027

(45) Tchakouté HK, Rüscher CH, Kong S, Kamseu E, Leonelli C. Geopolymer binders from metakaolin using sodium waterglass from waste glass and rice husk ash as alternative activators: A comparative study. Constr Build Mater. 2016 Jul;114:276–89. https://doi.org/10.1016/j.conbuildmat.2016.03.184

(46) Arellano-Aguilar R, Burciaga-Díaz O, Gorokhovsky A, Escalante-García JI. Geopolymer mortars based on a low grade metakaolin: Effects of the chemical composition, temperature and

aggregate:binder ratio. Constr Build Mater. 2014;50:642–8. https://doi.org/10.1016/j.conbuildmat.2013.10.023

(47) Hajimohammadi A, Provis JL, Van Deventer JSJ. The effect of silica availability on the mechanism of geopolymerisation. Cem Concr Res. 2011;41(3):210–6. https://doi.org/10.1016/j.cemconres.2011.02.001

(48) Tong KT, Vinai R, Soutsos MN. Use of Vietnamese rice husk ash for the production of sodium silicate as the activator for alkali-activated binders. J Clean Prod. 2018;201:272–86. https://doi.org/10.1016/j.jclepro.2018.08.025

(49) Lecomte I, Henrist C, Liégeois M, Maseri F, Rulmont A, Cloots R. (Micro)-structural comparison between geopolymers, alkali-activated slag cement and Portland cement. J Eur Ceram Soc. 2006;26(16):3789–97. https://doi.org/10.1016/j.jeurceramsoc.2005.12.021

(50) Nmiri A, Duc M, Hamdi N, Yazoghli-Marzouk O, Srasra E. Replacement of alkali silicate solution with silica fume in metakaolin-based geopolymers. Int J Miner Metall Mater. 2019;26(5):555–64. https://doi.org/10.1007/s12613-019-1764-2

(51) Villaquirán-Caicedo MA, Mejía de Gutiérrez R. Synthesis of ternary geopolymers based on metakaolin, boiler slag and rice husk ash. DYNA. 2015;82(194):104–10.

http://dx.doi.org/10.15446/dyna.v82n194.46352

(52) Onori R. Alkaline activation of incinerator bottom ash for use in structural applications. [Thesis PhD]. University of Rome XIII PhD Course in Environmental Engineering; 2011. Available in: https://gitisa.it/wp-content/uploads/tesi/2012/12-Tesi_Roberta_Onori.pdf

(53) Panagiotopoulou C, Kontori E, Perraki T, Kakali G. Dissolution of aluminosilicate minerals and by-products in alkaline media. J Mater Sci. 2006;42(9):2967–73. https://doi.org/10.1007/s10853-006-0531-8

(54) Xu Y, Jiang L, Xu J, Li Y. Mechanical properties of expanded polystyrene lightweight aggregate concrete and brick. Constr Build Mater. 2012;27(1):32–8. https://doi.org/10.1016/j.conbuildmat.2011.08.030

(55) Brás A, Leal M, Faria P. Cement-cork mortars for thermal bridges correction. Comparison with cement-EPS mortars performance. Constr Build Mater. 2013;49:315–27. https://doi.org/10.1016/j.conbuildmat.2013.08.006

(56) Turatsinze A, Bonnet S, Granju JL. Mechanical characterisation of cement-based mortar incorporating rubber aggregates from recycled worn tyres. Build Environ. 2005;40(2):221–6. https://doi.org/10.1016/j.buildenv.2004.05.012

(57) Medina NF, Medina DF, Hernández-Olivares F, Navacerrada MA. Mechanical and thermal properties of concrete incorporating rubber and fibres from tyre recycling. Constr Build Mater. 2017;144:563–73. https://doi.org/10.1016/j.conbuildmat.2017.03.196

(58) Raghavan D, Huynh H, Ferraris CF. Workability, mechanical properties, and chemical stability of a recycled tyre rubber-filled cementitious composite. J Mater Sci. 1998;33(7):1745–52. https://doi.org/10.1023/A:1004372414475

(59) Moreira A, António J, Tadeu A. Lightweight screed containing cork granules: Mechanical and hygrothermal characterization. Cem Concr Compos. 2014;49:1–8. https://doi.org/10.1016/j.cemconcomp.2014.01.012

(60) Sayadi AA, Tapia J V., Neitzert TR, Clifton GC. Effects of expanded polystyrene (EPS) particles on fire resistance, thermal conductivity and compressive strength of foamed concrete. Constr Build Mater. 2016;112:716–24.https://doi.org/10.1016/j.conbuildmat.2016.02.218

(61) Gong J, Duan Z, Sun K, Xiao M. Waterproof properties of thermal insulation mortar containing vitrified microsphere. Constr Build Mater. 2016;123:274–80. https://doi.org/10.1016/j.conbuildmat.2016.04.107

(62) Tamut T. Partial Replacement of Coarse Aggregates By Expanded Polystyrene Beads in Concrete. Int J Res Eng Technol.

2015;03(2):238–41.
https://doi.org/10.15623/ijret.2014.0302040

(63) Navarro F., Partal P, Martínez-Boza F, Valencia C, Gallegos C. Rheological characteristics of ground tire rubber-modified bitumens. Chem Eng J. 2002;89(1–3):53–61.
https://doi.org/10.1016/S1385-8947(02)00023-2

(64) Hall MR, Najim KB, Hopfe CJ. Transient thermal behaviour of crumb rubber-modified concrete and implications for thermal response and energy efficiency in buildings. Appl Therm Eng. 2012;33–34:77–85.
https://doi.org/10.1016/j.applthermaleng.2011.09.015

(65) Azimi EA, Mustafa M, Bakri A, Ming LY, Yong HC, Hussin K, et al. Processing and Properties of Geopolymers as Thermal Insulating Materials: A Review. Rev Adavanced Mater Sci. 2016;44:273–85.
https://doi.org/10.1016/j.applthermaleng.2011.09.015

(66) Moretti E, Belloni E, Agosti F. Innovative mineral fiber insulation panels for buildings: Thermal and acoustic characterization. Appl Energy. 2016;169:421–32.https://doi.org/10.1016/j.apenergy.2016.02.048.

(67) Najib NN, Ariff ZM, Bakar AA, Sipaut CS. Correlation between the acoustic and dynamic mechanical properties of natural rubber foam: Effect of foaming temperature. Mater Des. 2011;32(2):505–11.
https://doi.org/10.1016/j.matdes.2010.08.030

(68) Hansen CH. Fundamentals of Acoustics. University of Adelaide. 2019.

(69) Holmes N, Browne A, Montague C. Acoustic Properties of Concrete Panels with Crumb Rubber as a Fine Aggregate Replacement. Constr Build Mater. 2014;73:195–204.
https://doi.org/10.1016/j.conbuildmat.2014.09.107

(70) Arenas C, Luna-Galiano Y, Leiva C, Vilches LF, Arroyo F, Villegas R, et al. Development of a fly ash-based geopolymeric concrete with construction and demolition wastes as aggregates in acoustic barriers. Constr Build Mater. 2017;134:433–42.
https://doi.org/10.1016/j.conbuildmat.2016.12.119

(71) Acoustic C. Commercial Acoustic. 2019. Available from: https://commercial-acoustics.com/product/acoustic-absorption-panel/

(72) Tiwari V, Shukla A, Bose A. Acoustic properties of cenosphere reinforced cement and asphalt concrete. Appl Acoust. 2004;65(3):263–75.
https://doi.org/10.1016/j.apacoust.2003.09.002